

Influence of Manganese doping on Structural, optical and ethanol sensing of SILAR synthesized CuO thin film

Basudeb Roy Chaudhury

Department of B.Ed, Bijoy Krishna Girls'College, Howrah-711 101 West Bengal, India. Pin: 711 101.

Abstract - In this report, we have primarily studied the influence of manganese incorporation on structural, optical and ethanol sensing properties of copper oxide (CuO) thin films synthesized by successive ion layer adsorption and reaction (SILAR) technique. The materials have been characterized using X-ray diffraction and optical properties were measured by UV-VIS spectrophotometric. Reduction in grain size in doped films up to a certain extent of doping (tentatively 5%) were confirmed from XRD analysis, beyond which there is a reverse tendency. Increase in band gap in doped films were observed up to 5% doping level which could be associated with enhanced carrier density in doped films. Maximum sensitivity of 87% in the presence of 1500 ppm ethanol at the operating temperature $180^{\circ}C$ was obtained for 5% doped film.

Keywords: CuO thin film; SILAR; Optical band gap; Ethanol sensitivity.

1. INTRODUCTION

Nanostructured cupric oxide (CuO) is one of the important transition metal oxide semiconductor materials having unique optical and electrical properties. CuO has demonstrated its potential in solar cell [1], gas sensor [2-4], superconducting material [5-6], magnetic storage devices [7] and photovoltaic devices [8]. The narrow band gap of CuO at ~ 1.2 eV makes it useful for photoconductive and photothermal applications and as an antibacterial agent [9]. Accordingly, besides its abundance distribution, chemical stability and environmental friendliness, CuO nanostructures have attracted considerable attention due to its interesting electrical and optical properties [10]. Various researchers have reported these properties for CuO and doped CuO thin films. The p -type conductivity is believed to be due to generation of cation vacancies in the CuO structure [11]. The p -type oxides have a tendency to exchange lattice oxygen with air and this is useful in maintaining stoichiometry of the oxides. Another advantage of p -type oxides is that

the temperature dependence of conduction in high-temperature range is considerably less than that of n -type oxides. The physical and chemical properties of CuO thin film can be affected by doping in terms of the resulting optical, electrical, and structural properties. Influence of various dopants such as zinc (Zn), lead (Pb), lithium (Li) and iron (Fe) on structural, morphological and optical properties of CuO has been reported by various groups [12-15]. Zinc and Nickel doping has been reported to influence the ferromagnetic properties of CuO , the extent of which depends on the amount of dopant ions. Ismail et al, [16] present structural properties of Mn-doped CuO thin films prepared by chemical spray pyrolysis technique. Rahman et al. [17] studies band gap tuning and p to n -type transition in Mn-doped CuO nanostructured thin films. Zhu et al. [18] describes in their work to structural and magnetic properties of Mn-doped CuO thin films, Mustafa et al presents preparation Doped CuO Thin Film and Studies of Its Antibacterial Activity. There is not any report the doping effect on ethanol sensitivity in CuO thin film of manganese ion. Out of number of chemical techniques, CBD is one through which films of thin layers of uniform thickness can be coated on large area. The technique is relatively simple and economic for mass production processes. We have actually adopted successive ion layer adsorption and reaction (SILAR) technique in this work to synthesize Mn: CuO thin films which is a modified version of CBD. Both SILAR and CBD involve the same principle where film formation takes place through ion-by-ion deposition of cations and anions on nucleating sites on the immersed surfaces. While in CBD, deposition of thin films occurs due to substrate maintained in contact with dilute chemical baths containing cationic and anionic solutions together, in SILAR, deposition occurs by immersing the substrate in separately placed cationic and anionic precursors. The only common problem in CBD is precipitate formation and wastage of material since the ions combine to form nuclei in the solution also, apart from the substrate. This is avoided in SILAR [8]. Also doping with metal ions at low temperatures can be conveniently carried out using SILAR technique.

In view of this, the present work was taken up primarily to study the influence on Mn doping on structural, optical and ac electrical conductivity in SILAR synthesized CuO thin film. Thus, in the present study, we have successfully synthesized $Cu_{1-x}Mn_xO$ ($x = 0.00, 0.01, 0.03, 0.05$ and 0.07) thin films by SILAR method. The effect of different doping concentrations of Mn on structural, optical, ethanol sensing properties of CuO thin film has been investigated and compared with those for undoped CuO thin films.

2. EXPERIMENTAL

CuO thin film was deposited on microscope glass slide substrates cleaned prior to deposition. The substrate was kept overnight in freshly prepared chromic acid solution which was followed by rinsing in distilled water and finally ultrasonic cleaning in equivolume mixture of acetone and alcohol. It was alternately dipped in a cationic precursor of copper thiosulphate complex and an anionic precursor of 1.0 M potassium hydroxide solution (KOH). The copper thiosulphate complex was prepared by adding sodium thiosulphate ($Na_2S_2O_3$) in copper sulphate ($Cu_2SO_4 \cdot 5H_2O$) until a colorless solution results. The cleaned substrate was first dipped in hot KOH solution maintained at $70^\circ C$ using a constant temperature bath and then dipped in copper complex solution kept at room temperature. The dipping time in each bath was 5 seconds and 25 such dipping cycles were performed to get a uniform thin film. One complete set of dipping involves dipping of the substrate in cationic and anionic precursor respectively. The reaction between Cu^{2+} ion and OH^- ion takes place on the substrate surface leading to the formation of Cu_2O thin film [19] which on subsequent heat treatment in air at $400^\circ C$ leads to the formation of CuO film. A thin blight brown adhesive film was formed on the substrate. Manganese doping was carried out by adding appropriate amount of manganese sulphate in cationic precursor.

The phase identification and crystalline properties of the samples were studied by X-ray diffraction (XRD) method with the help of a Bruker (D8 advance) x-ray diffractometer using Ni-filtered CuK_α radiation ($\lambda = 1.5418 \text{ \AA}$). The diffraction data were recorded in the angular range $20^\circ - 80^\circ$ and the experimental peak positions were compared with standard Joint Committee of Powder Diffraction System (JCPDS) files and Miller

indices were assigned to the peaks. The surface morphology study was performed using FESEM. The absorbance data was measured using double-beam spectrophotometer (Shimadzu, UV-1800) at room temperature. The band gap of the films was calculated from the absorption edge of the spectrum. Gas-sensing experiments were carried out by placing the sample in a test chamber made of glass. Copper wires with conducting silver paste were used for the electrode. Temperature variation was recorded using a sensitive thermocouple placed inside the closed glass test chamber. Change of electrical resistance in the presence of the target gas was measured using at Keithley 6514 DMM set-up. Requisite amounts of the target gas were passed over the sample using a regulated flow meter (flow rate of 1 L per min).

3. RESULT AND DISCUSSION

3.1 Structural analysis

Figure 1 shows the XRD patterns of CuO and Mn doped CuO thin films. Prominent diffraction were peaks observed at $\sim 35.94^\circ$ and $\sim 39.16^\circ$ corresponding to (-111) and (111) diffraction planes which can be associated with monoclinic copper oxide [JCPDS file no. 89-5899]. The other minor peaks at $\sim 32.53^\circ, 49.32^\circ, 54.21^\circ, 58.82^\circ, 62.21^\circ, 66.67^\circ, 68.48^\circ$ and 75.51° also compares well with monoclinic CuO . The corresponding diffraction planes are (110), (20-2), (020), (202), (11-3), (31-1), (220) and (22-2) respectively. The crystallite size was calculated using Scherrer's formula [20]:

$$D = \frac{k\lambda}{\beta \cos \theta}$$

where k is the Scherrer constant, β is the full width at half maximum (FWHM) intensity of the diffraction peak for which the particle size is to be calculated, θ is the diffraction angle of the concerned diffraction peak and λ is the wavelength of X-ray used. The average value of crystallite size estimated was found to decrease from $\sim 37.1 \text{ nm}$ for CuO to $\sim 25.4 \text{ nm}$ for 5% $Mn : CuO$. The value was however found to increase to $\sim 26.6 \text{ nm}$ for 5% $Mn : CuO$. It is apparent from the figure that the diffraction peaks get broadened with enhancement in doping level up to 5%, above which there is a reduction in width of the diffraction peak. Thus, the particle size decreases up to a certain level of Mn incorporation, above which there is a reverse tendency.

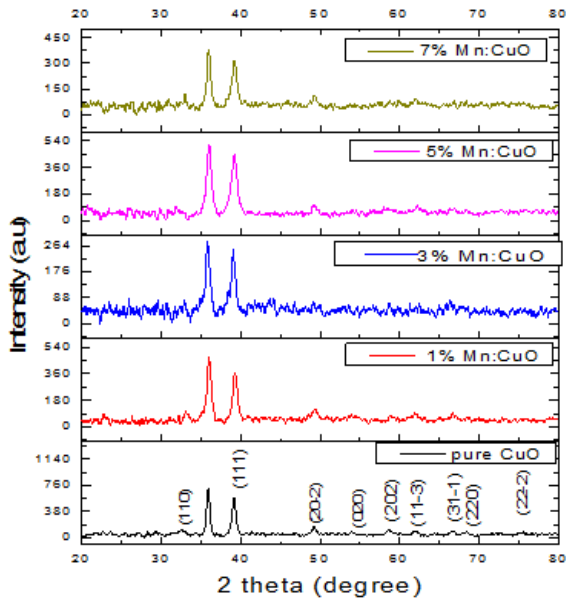


Fig-1: X-ray powder diffraction patterns of of CuO and Mn doped CuO thin film

In order to find a possible reason behind such enhancement in particle size, the average microstrain (ϵ) in the films were determined using of the formula [20]:

$$\epsilon = \frac{\beta \cos \theta}{4}$$

Figure 2 shows the variation of average microstrain and particle size of the samples with doping and they are found to vary in an opposite manner to each other. The strain was found to increase from $\sim 3.72 \times 10^{-3}$ for CuO to $\sim 6.82 \times 10^{-3}$ for 5% doping and then was found to trim down to $\sim 6.15 \times 10^{-3}$ for 7%. Mn : CuO Accordingly the reduction of particle size up to 5% doping level might be due enhanced strain leading to enhanced polycrystallinity in the samples.

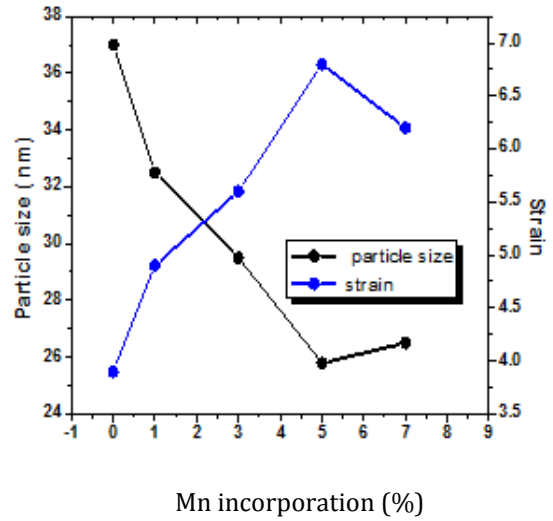
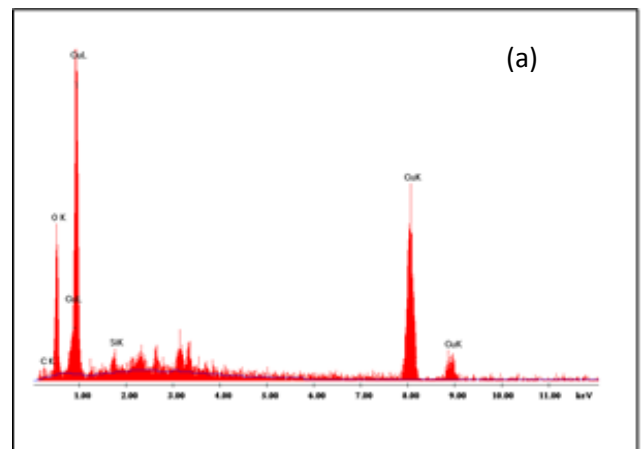


Fig -2: Variation of grain size and micro strain CuO and Mn : CuO thin films

Incorporation of Ni was also confirmed from EDX measurement. Figure 3(a) shows the EDX pattern of pure CuO and 3(b) for 5% Mn doped CuO film. EDX spectrum confirmed the presence of Cu, O and Mn elements in the deposited film. Some amount of Si was found to be present which appears from the glass substrate used for film deposition.



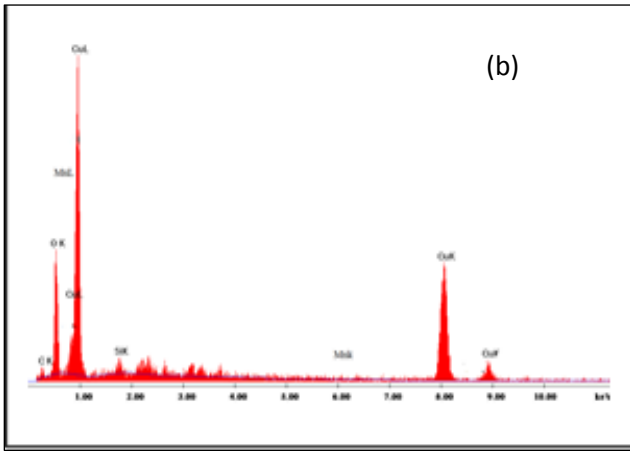


Fig- 3: (a) and (b) shows EDX pattern of *CuO* and *Mn : CuO* thin films

3.2. Optical study

Figure 4 (a) shows the plot of absorbance as a function of wavelength for pure and doped *CuO* thin films in the wavelength range 400-1000 nm. Band gap energy (E_g) was derived from the mathematical treatment of the data obtained from the absorbance vs. wavelength for direct band gap *CuO* [21] using the following relationship:

$$(\alpha h\nu)^2 = A(h\nu - E_g)$$

where ν is the frequency and h is the Planck's constant. A is a temperature independent constant for a direct band gap semiconductor and temperature dependent constant for an indirect band gap one. For direct band gap semiconductor, this is given by [22]:

$$A = \frac{4\pi c \sigma_o}{n_o E_u}$$

where σ_o is the electrical conductivity at absolute zero, n_o is the refractive index and E_u is the Urbach energy. The energy intercept of the plots of $(\alpha h\nu)^2$ versus photon energy $h\nu$ yields E_g for direct transition as shown in figure 4(b). The value of band gap was found to increase with increasing dopant concentration up to 6% doping level. Beyond this level of doping, the band gap was found

to decrease. The observed values were ~ 1.61 eV for *CuO* and it increased to ~ 1.95 eV for 5% Mn doping. The value however decreased with further Mn incorporation and it was ~ 1.86 eV for 7% Zn doping. The band gap values were an average of three measurements in different areas of the film. There was a dispersion of ~ 0.02 eV about the observed value. The observed result is in contrast to that reported for Mn incorporated *CuO* thin films where doping has been reported to reduce the band gap. Rahman et al. [17] on the other hand reported a decrease in band gap in *CuO* nanoparticles due to Mn doping. Although no such report on Mn doped *CuO* thin films is reported in the literature to the best of our knowledge, such an observation of band gap enhancement with increasing doping level might be due to familiar Burstein-Moss effect [23,24] where carrier density is increased due to dopant incorporation in host semiconductor. Such an effect has been observed for *Ni* doped *CdO* films [25] and *In* doped *CuO* [26]. This also indicates that manganese ions substitute copper ions in the lattice structure up to a certain level of doping. Decrease in band gap beyond a certain level of doping might be due to excess manganese ions going to interstitial sites (instead of substitutionally replacing copper ions in the lattice sites).

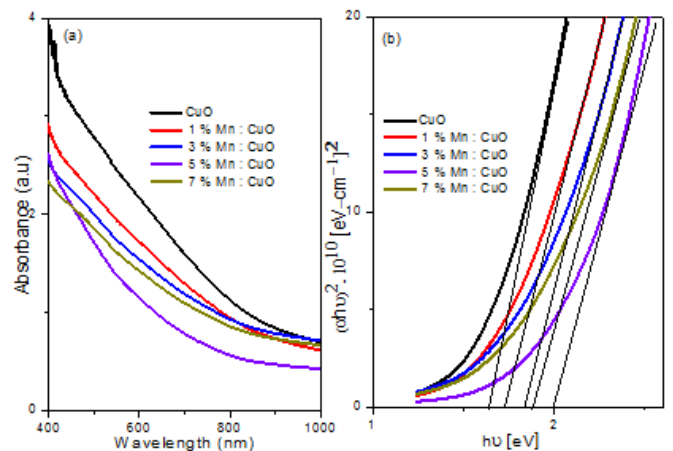
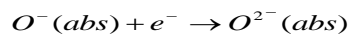
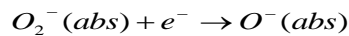
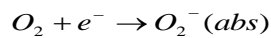


Fig -4: (a) Absorbance spectrum of *CuO* and doped *CuO* thin films; (b) Plot of $(\alpha h\nu)^2$ vs. $h\nu$ for *CuO* and *Mn : CuO* thin films

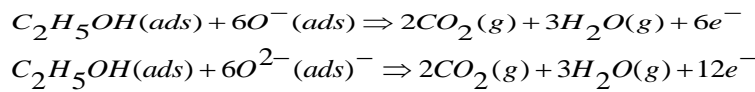
3.3. Gas Sensing Characteristics

The gas sensing characteristics for fixed concentration of 500 ppm ethanol gas in air was carried

out for all samples. Fig. 5 the variation of percent sensitivity ($S\%$) as a function of temperature. The performance of CuO thin film as a gas sensor is related to the changes in electrical resistance induced by adsorption/desorption of the target gas molecules on its surface. As air is exposed on film surface, oxygen molecule gets absorbed on the sensor surface leads to formation of oxygen ion species such as O_2^- , O^{2-} and O^- ions by trapping electron from conduction band and effectively decrease resistance of the CuO film sensor (increase conductivity). This reaction can be represented as



Now when ethanol (reducing gas) is exposed to the sensing film surface, ethanol molecules interact with chemisorbed oxygen species and releasing electrons that recombine with holes as a result decrease electrical conductance which in turn increase the sensor resistance. This mechanism is known as the ionosorption model [27] and the sensing reaction is given by;



Percent sensitivity ($S\%$) of the thin film sensor is defined as

$$S\% = \frac{R_{air} - R_{gas}}{R_{air}} \times 100$$

where R_{air} is the resistance of the sample in air and R_{gas} is the resistance in presence of target gas. The maximum sensitivity has been achieved at much lower operating temperature of 180°C for 5% doped film thin films. The grain size of the CuO sensor is in the order of few nm, so sensing body consists of pores between the grains. Transport of gas between the pores occur accordingly to Knudsen diffusion equation [28]

$$D = \frac{3r}{(2RT/\pi M)^{1/2}}$$

where r is the pore radius, M the molecular weight of the gas, R the gas constant and T the temperature.

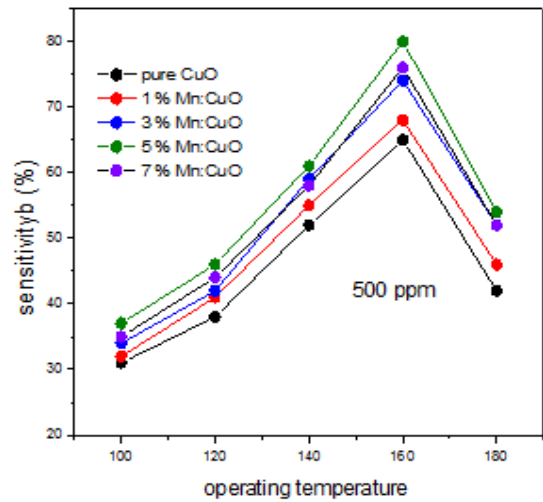


Fig- 5: the variation of percent sensitivity ($S\%$) as a function of temperature for all set of deposited films of CuO

When ethanol vapor gas exposed on surface thin film chemisorbed oxygen ion species interact with ethanol molecules and thereby releasing electron which recombine with holes to decrease electrical conductivity. So, it is clear gas sensing is directly proportional to grain size. Moreover, increase in porosity due to cauliflower structure increases the effective surface area as a results reaction of target gas molecules with chemisorbed species increases. As the 30-dipping cycle deposited CuO thin film shows more crystalline with highest grain size and high porosity comparable to others so it shows highest response for ethanol sensing. Temperature dependence of the sensing material i.e., maximum sensing response at operating temperature (180°C) can be understood as follows: at lower temperatures the absorbed ethanol molecule has not get enough energy to overcome the activation energy barrier to react with absorbed oxygen species and at high temperatures gas absorption is too difficult as surface reactivity increased adequately in that temperature. Thus at some in-between temperature sensor performance is reaches maximum value [29]

Fig. 6 shows the response and recovery characteristics of 5% doped film at operating temperature in presence of different concentration ethanol gas. Before the target gas is exposed, the sensor material is permitted to equilibrate in air at the operating temperature for a certain period of time. As soon as target gas is exposed, the resistance increases very sharply initially and then

increases slowly to reach saturation value (R_{gas}) when reaction between chemisorbed oxygen species and target gas molecules is complete [30]. Fig 6 shows the gas sensing performance increase with increase of concentration of target gas and maximum sensitivity is observed at 1000 ppm, for further increase of gas concentration up-to 1000ppm sensitivity remains almost constant. The enhancement in sensitivity with concentration can be explained from the fact that higher concentration of target gas implies higher number of reactants available for surface reaction and further increase of concentration saturates number of reactants become saturate which in turn saturate sensitivity. The observed response time (time taken for 90% of total resistance reduction after gas is on) is ~ 50 sec and the recovery time (recovering the initial resistance after gas is off) is ~85sec. The overall sensing performance of the deposited film is good comparable with previous reported literature [31]. Although no systematic results were generated for ammonia and acetone, the material was found to be very low sensitive to 1000 ppm ammonia (8%) and acetone (5%) at maximum operating temperature.

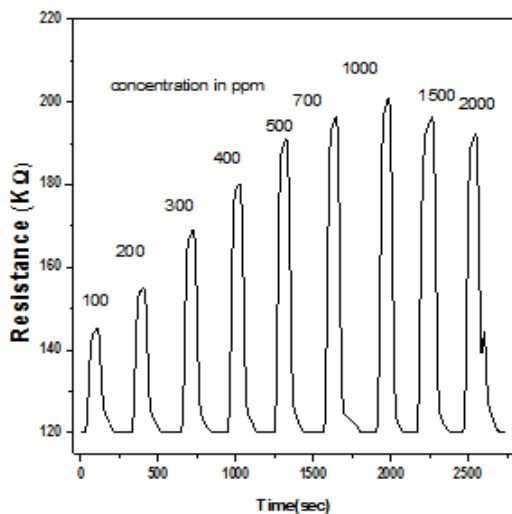


Fig- 6: shows the response and recovery characteristics of 5% Mn doped CuO thin film at operating temperature in presence of different concentration ethanol gas.

4. CONCLUSIONS

In the presented work, we have primarily reported the influence of Mn incorporation on ac electrical conductivity, dielectric relaxation mechanism and impedance spectroscopy characteristics of *CuO* thin films

synthesized by SILAR technique. Manganese could be successfully doped in *CuO* thin film by this technique. The structural, optical and electrical characteristics of the films were found to be a sensitive function of doping level. Decrease in grain size and enhancement in disorder was found from XRD analysis up to 5% doping, beyond which there is a reverse tendency. Similarly, the band gap in doped films also shows inflexion at this particular level of Mn incorporation. The band gap increase with up to this particular level of doping and then decreases. Incorporation of Mn was confirmed from EDX measurements. 5% Mn doped CuO film shows excellent gas sensing ability with 87% sensitivity for 1000 ppm ethanol at much lower operating temperature of 180°C.

REFERENCES

- [1] K, Han K and M Tao, "Electrochemically deposited p-n homojunction cuprous oxide solar cells," *Sol Energy Mater Sol Cells* vol. 93, 2009, pp. 153-157.
- [2] S Steinhauer, E Brunet, T Maier, G Mutinati, A Kock, O Freudenberg, C Gspan, W Grogger, A Neuhold, R Resel, "Gas sensing properties of novel CuO nanowire devices," *Sensors and Actuators B* vol. 187, 2013, pp. 50-57.
- [3] Katti V, Debnath A, Muthe K, Kaur M, Dua A, Gadkari S, Gupta S, Sahni V (2003) Mechanism of drifts in H₂S sensing properties of SnO₂: CuO composite thin film sensors prepared by thermal evaporation. *Sensors and Actuators B* 96:245-252
- [4] Zoolfakar AS, Ahmad MZ, Rani RA, Ou JZ, Balendhran S, Zhuiykov S, Latham K, Wlodarski W, Zadeh KK (2013) Nanostructured copper oxides as ethanol vapour sensors, *Sensors and Actuators B* 185:620- 627
- [5] Zheng X, Xu C, Tomokiyo Y, Tanaka E, Yamada H, Soejima Y (2000) Observation of charge stripes in cupric oxide, *Phys Rev Lett* 85:5170-5173
- [6] Tokura Y, Takagi H, Uchida S (1989) A superconducting copper oxide compound with electrons as the charge carriers. *Nature* 337:345-347
- [7] Fan H, Yang L, Hua W, Wu X, Wu Z, Xie S, Zou B (2014) Controlled synthesis of monodispersed CuO nanocrystals. *Nanotechnology* 15:37-42
- [8] Jayakrishnan R, Kurian AS, Nair VG, Joseph (2016) MR Effect of vacuum annealing on the photoconductivity of CuO thin films grown using sequential ionic layer adsorption reaction. *Mat Chem Phys* 180:149-155

- [9] Yousef A, Barakat NA, Amna T, Al-Deyab SS, Hassan MS, Hay AA, Kim HY (2012) Inactivation of pathogenic *Klebsiella pneumonia* by CuO/TiO₂ nanofibers: A multifunctional nanomaterial via one-step electrospinning. *Ceram Int* 38:4525-4532
- [10] Khmissi H, Sayed AME, Shaban M (2016) Structural, morphological, optical properties and wettability of spin-coated copper oxide; influences of film thickness, Ni, and (La, Ni) co-doping. *J Mater Sci* 51:5924-5938
- [11] Wang C, Fu XQ, Xue XY, Wang YG, Wang TH (2007) Surface accumulation conduction controlled sensing characteristic of p-type CuO nanorods induced by oxygen adsorption. *Nanotechnology* 18:145506-14510
- [12] Sonia S, Annsi IJ, Suresh PS, Mangalaraj D, Viswanathan C, Ponpandian N (2015) Hydrothermal synthesis of novel Zn doped CuO nanoflowers as an efficient photo degradation material for textile dyes. *Mater Lett* 144:127-130
- [13] Chand P, Gaur A, Kumar A, Kumar UG (2014) Structural and optical study of Li doped CuO thin films on Si (100) substrate deposited by pulsed laser deposition. *Appl Surf Sci* 307:280-286
- [14] Bayansal F, Gulen Y, Sahin B, Kahraman S, Cetinkara H (2015) CuO nanostructures grown by the SILAR method: influence of Pb-doping on the morphological, structural and optical properties. *J Alloy Compd* 619:378-382
- [15] Basith NM, Vijaya JJ, Kennedy LJ, Bououdina M (2013) Structural, optical and room-temperature ferromagnetic properties of Fe-doped CuO nanostructures. *Physica E Low Dimens Syst Nanostruct* 53:193-199
- [16] Ismail MJ, Khodair ZT, Mahmood MK (2021) structural properties of Mn-doped CuO thin films prepared by chemical spray pyrolysis technique. *Materials Today: Proceedings*. 49: 3558-3567.
- [17] Rahaman R, Sharmin M, Podder J (2022) Band gap tuning and p to n-type transition in Mn-doped CuO nanostructured thin films[J]. *J. Semicond*, 43(1).
- [18] Zhu H, Zhao F, Pan L, Zhang Y, Fan C (2007) Structural and magnetic properties of Mn-doped CuO thin films, *Appl. Phys.* 101, 09H111.
- [19] Mustafa AH, Sadeer MM, Duha SA (2018) Preparation Doped CuO Thin Film and Studies of Its Antibacterial Activity, *ACTA PHYSICA POLONICA A* 135(4).
- [20] M. Dhanam, R. P. Rajeev, P. K. Manoj, *Mater. Chem. Phys.* **107**, 289 (2008)
- [21] Balamurugan B, Mehta BR (2001) Optical and structural properties of nanocrystalline copper oxide thin films prepared by activated reactive evaporation. *Thin solid films* 396:90-96
- [22] Sayed AM, Morsi WM (2013) Dielectric relaxation and optical properties of polyvinyl chloride/lead monoxide nanocomposites. *Polym Compos* 34:2031-2039.
- [23] Burstein E (1954) Anomalous optical absorption limit in InSb, *Phys Rev* 93:632
- [24] Mondal S, Bhattacharyya SR, Mitra P (2013) Effect of Al doping on microstructure and optical band gap of ZnO thin film synthesized by successive ion layer adsorption and reaction. *Pramana J Phys* 80:315-326
- [25] Yakuphanoglu F (2011) Preparation of nanostructure Ni doped CdO thin films by sol gel spin coating method. *J Sol-Gel Sci Technol* 59:569-573
- [26] Yildiz A, Horzum S, Serin N, Serin T (2014) Hopping conduction in In-doped CuO thin films. *Appl Surf Sci* 318:105-107
- [27] Saaédi A, Yousefi R (2007) Improvement of gas-sensing performance of ZnO nanorods by group-I elements doping, *J. Appl. Phys.* 122
- [28] Terry PA, Anderson M, Tejedor I (1999) Catalytic dehydrogenation of cyclohexane using coated silica oxide ceramic membranes, *J. Porous Mater.* 6 267-274.
- [29] Liu J, Wang X, Peng Q, Y. Li (2005) Vanadium pentoxide nanobelts: Highly selective and stable ethanol sensor materials, *Adv. Mater.* 17 764-767.
- [30] Zoolfakar AS, Ahmad MZ, Rani RA, Ou JZ, Balendhran S, Zhuiykov S, Latham K, Wlodarski W, Kalantar-Zadeh K (2013) Nanostructured copper oxides as ethanol vapour sensors, *Sensors Actuators, B Chem.* 185 620-627.
- [31] Gopalakrishna D, Vijayalakshmi K, Ravidhas C (2013) Effect of annealing on the properties of nanostructured CuO thin films for enhanced ethanol sensitivity, *Ceram. Int.* 39, 7685-7691.